

Structural Studies of Multifunctional SrTiO₃ Nanocatalyst Synthesized by Microwave and Oxalate Methods: Its Catalytic Application for Condensation, Hydrogenation, and Amination Reactions

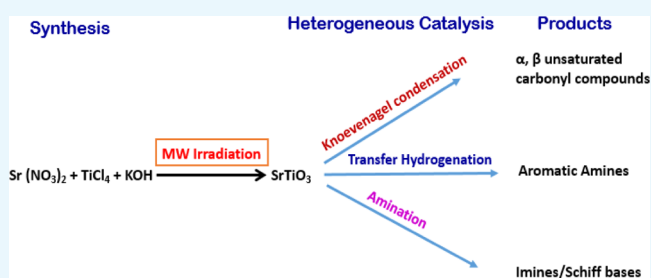
Chilukoti Srilakshmi,^{*,†,‡} Rohit Saraf,[†] and Chikkadasappa Shivakumara[†]

[†]Solid State and Structural Chemistry Unit (SSCU), Indian Institute of Science (IISc), C.V. Raman Road, 560012 Bengaluru, Karnataka, India

[‡]Department of Chemistry, GITAM University, Nagadenahalli, Doddaballapur Taluk, 562163 Bengaluru, Karnataka, India

ABSTRACT: The present study deals with the synthesis of SrTiO₃ (STO) nanocatalysts by conventional oxalate and microwave-assisted hydrothermal methods. Thorough characterization of the nanocatalysts synthesized has been done by using various techniques such as X-ray diffraction (XRD), Fourier transform infrared spectroscopy, N₂ physisorption, transmission electron microscopy, total acidity by pyridine adsorption method, and acidic strength by *n*-butylamine potentiometric titration, respectively. Structural parameters were estimated by Rietveld refinement analysis from XRD

data which confirms cubic structure of SrTiO₃. Traces of impurities such as TiO₂ and SrCO₃ were found in conventional catalysts, whereas these are absent in microwave catalyst. Brunauer–Emmett–Teller (BET) surface area of the microwave catalyst was enhanced 14-folds compared to conventional catalyst. Increase in Lewis acid sites and their strength were also observed in STO microwave catalyst. Catalytic performance of the catalysts was evaluated for various reactions, such as Knoevenagel condensation of benzaldehyde, catalytic transfer hydrogenation of nitrobenzene, and amination of benzaldehyde. Catalytic results reveal that microwave-synthesized catalyst showed 100% conversion and selectivity (>99% yield) for the chosen reactions than the conventional catalyst. Excellent catalytic activity of the STO microwave catalyst was due to high BET surface area, pore volume, and acidity of the catalyst, as compared to conventional catalyst. The present study marks the first-time application of perovskite-based SrTiO₃ as a potential multitasking cost-effective catalyst for the above reactions and synthesized using environment friendly microwave synthesis method.



INTRODUCTION

The escalating demand for environmental friendly products and process leads to the development of nanocatalysts that provide high selectivity and activity in various chemical reactions.^{1–3} Multitask catalysts are catalysts which could be able to catalyze at least two consecutive reactions.⁴ However, retention of their selectivity and reusability after several reaction cycles is very challenging.⁵ During the past few years, various catalysts have been exploited for diverse chemical reactions such as Lewis acids,⁶ amine-functionalized solid supports,⁷ ionic liquids,⁸ zeolites,^{9,10} and metal organic frameworks.^{5,11} However, these catalysts offer several disadvantages such as utilization of hazardous and carcinogenic solvents, large amount of catalysts, long reaction time, nonrecoverable catalysts, and generation of secondary products that hindered their large-scale industrial application.^{12,13} Therefore, it is highly desirable to develop efficient recoverable solid-phase catalyst that can overcome these problems and show high activity as well as maximum reusability. Hence, in the present study, we have explored an alternate perovskite as a catalyst for three different types of catalytic reactions.

Structure of perovskites and their physical and chemical properties were discussed in our previous publication.¹⁴ Among various perovskites, much attention has been paid to SrTiO₃ because of its structural, electrical, optical, and catalytic properties, which can be tailored for practical applications. Many methods have been reported for synthesizing titanates such as coprecipitation,¹⁵ solid-state reaction,¹⁸ liquid–solid reaction method,¹⁶ molten salt synthesis,¹⁷ sol–gel,¹⁸ and hydrothermal method.¹⁹ Recently, we have explored oxalate route²⁰ and microwave-assisted hydrothermal (MH) method for the synthesis of BaTiO₃ and Cr-doped BaTiO₃ nanocatalysts.¹⁴ The present work is in continuation of this previous work to identify the most active catalyst than microwave-synthesized BaTiO₃, and its applicability for multitasking in various reactions has been explored.

Microwave chemistry is emerging as a viable alternative green chemistry and provides a more sustainable method for

Received: June 6, 2018

Accepted: August 21, 2018

Published: September 5, 2018

the synthesis of nanomaterials in the future. It has been considered green because the environmental-friendly solvents (e.g., water and ionic liquids) have often been applied in combination with microwave heating method. On the other hand, conventional oxalate (CO) route offers advantages in terms of better structural composition and ease of the process. However, microwave heating has several advantages in comparison with conventional synthesis methods such as less synthesis time, and limited use of solvents makes the process clean; require less temperature for synthesis, uniform heating, high heating rate, phase purity of products, less expensive, and high-energy efficiency.¹⁰ Whereas conventional synthesis method requires extended period of time and consumes lot of energy. From an industrial point of view, such synthesis method is not environmentally and economically viable.

Knoevenagel condensation of aldehydes is widely used to synthesize α , β -unsaturated carbonyl compounds which were used as intermediates or end products in pharmaceuticals, perfumes, polymers, and agrochemical industries.^{21,22} Several catalysts such as organic bases, Lewis acids, ionic liquids, metal–organic frameworks, and so forth, have been used for Knoevenagel condensation reaction.^{23–26} The reduction of nitro compounds to the corresponding amines is very important as nitroarenes and their derivatives cause pollution, and these are mainly formed during the production of synthetic dyes, pesticides, herbicides, and insecticides.²⁷ Amination of aromatic aldehydes is one of the important route for the synthesis of imines and their derivatives which are important organic intermediates in the synthesis of pharmaceuticals and agrochemicals.²⁸ In the literature, several methods described the synthesis of imines.^{28–30} However, most of the catalysts used for these reactions have disadvantages such as not being environmentally friendly, excess starting materials, scarcity of the metals, formation of unavoidable byproducts, and most importantly narrow substrates scope.

In the current article, we have employed SrTiO₃ nanocatalyst as the green catalyst for Knoevenagel condensation, catalytic transfer hydrogenation, and amination reactions. The catalysts were synthesized via microwave hydrothermal method and CO methods, and the effect of synthesis method on the catalytic activity of the catalysts has been investigated. The nanocatalysts synthesized were characterized by various advanced analytical techniques. Further, SrTiO₃ was used for the first time for a variety of reactions and recyclability of the same in the chosen reactions.

Characterization Techniques. The nanocatalysts that are synthesized were thoroughly characterized by using the following techniques and their details are as follows: powder X-ray diffraction (XRD) using PAN analytical X'pert PRO Powder Diffractometer with Cu K α ($\lambda = 1.5418 \text{ \AA}$) as the radiation source.

Fourier transform infrared (FTIR) spectra were measured in the wavenumber range of 4000–350 cm⁻¹ at ambient temperature by PerkinElmer FTIR-300 spectrometer using KBr pellet method.

The Brunauer–Emmett–Teller (BET) surface area measurements were performed using Quantachrome Autosorb iQ₂ automated gas sorption analyzer. Samples are pretreated in N₂ at 300 °C for 4 h, before adsorbing N₂ at liquid nitrogen temperature (–196 °C), and the BET surface area and pore volume of the catalysts were obtained by N₂ adsorption and desorption isotherms. The particle size and morphology were

studied using a transmission electron microscope (Model JEM-2010, JEOL, Tokyo, Japan).

Acidic strength of the catalyst powders was determined by *n*-butylamine potentiometric titration method. About 0.5 g of the solid was stirred in acetonitrile for 3 h, and the contents were titrated with a solution of 0.01 N *n*-butylamine in acetonitrile at a flow rate of 0.02 mL/min; the variation in the electrode potential was measured with a potentiometric titrator using a standard calomel electrode. This method allows the determination of the total number of acidic sites and their strength. For interpretation of the results, the initial electrode potential (E_i) is taken as the maximum acidic strength of the surface sites and the range, where the plateau reached (mequiv/g) is considered as the total number of acid sites.³¹ The acidic strength of the surface sites can be assigned according to the following ranges very strong site $E_i > 100 \text{ mV}$; strong site $0 < E_i < 100 \text{ mV}$; weak site $-100 < E_i < 0 \text{ mV}$; very weak site $E_i < -100 \text{ mV}$.

Total acidity was determined using pyridine adsorption method, and the changes were recorded by FT-IR spectroscopy. Prior to pyridine, adsorption samples were degassed at 120 °C for 1 h and then saturated with pyridine and then evacuated at 115 °C for 30 min to remove any physisorbed pyridine. FT-IR spectra of the samples were then recorded in the wavenumber range of 1200–1800 cm⁻¹.

Catalytic Activity. The Knoevenagel condensation reaction of benzaldehyde with ethyl cyanoacetate to form ethyl *trans*- α -cyanocinnamate was carried out by taking 20 mmol of benzaldehyde and 20 mmol of ethyl cyanoacetate and 10 mL of water as a solvent in a 100 mL round-bottom flask. Then, 120 mg of catalyst was added to the reaction mixture and stirred under reflux conditions at 80 °C for 30 min in a silicon oil bath.

Catalytic reduction of nitrobenzene to aniline was carried out using hydrazine hydrate as hydrogen donor in a two-necked 100 mL round-bottom flask fitted with a reflux condenser. In a typical run, 80 mg of the catalyst was placed in a solution containing 10 mmol of nitrobenzene, 10 mmol of KOH pellets, 1.5 mL of hydrazine hydrate, and 10 mL of 2-propanol. The mixture was continuously stirred and refluxed at 80 °C for 2–6 h in an oil bath.

Catalytic amination was conducted under continuous stirring in a two-necked 50 mL round-bottom flask fitted with a reflux condenser. The catalyst (120 mg) was dispersed in a solution containing 2 mmol of benzaldehyde and 2 mmol of aniline in 2 mL of toluene, and the contents of the flask were stirred and refluxed at 110 °C for 24 h in an oil bath. The analysis of the above three reaction samples was done by withdrawing definite aliquots of the reaction sample at regular intervals and analyzed them using GC-MS (Thermo Trace GC Ultra (GC), Thermo DSQ II (MS); with DB5 MS column of 30 mL \times 0.25 mm ID \times 0.25 μm film thickness and with electron multiplier detector).

Recycling of Catalysts. Catalysts were recycled after every catalytic reaction. The catalyst was separated by centrifugation, washed with ethanol, and dried in an oven at 120 °C overnight before using it in the next reaction.

RESULTS AND DISCUSSION

Powder XRD. The diffraction patterns of STO nanocatalysts synthesized by both conventional (STO_C) and microwave (STO_M) methods are shown in Figure 1. XRD patterns were indexed to SrTiO₃ cubic perovskite structure

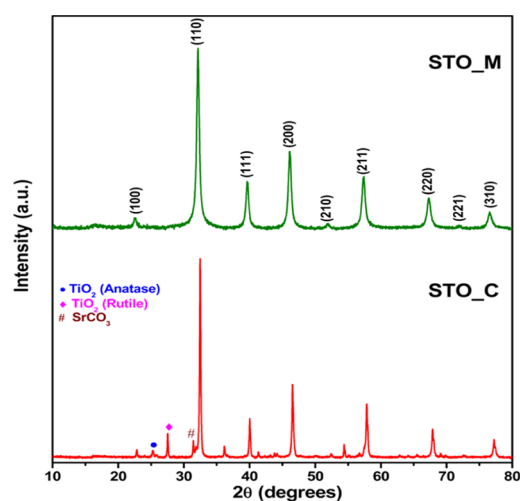


Figure 1. Powder XRD patterns of STO nanocatalysts synthesized by the conventional and microwave methods.

with $Pm\bar{3}m$ (no. 221) space group (JCPDS card no. 073-0661) in both STO_C and STO_M catalysts. Secondary phases corresponding to TiO_2 and $SrCO_3$ are present in STO_C, whereas in STO_M, pure phase has been observed without any traces of impurities. This study reveals that a single pure phase should be obtained using the MH method. Further, the peak broadening was observed in STO_M, which is the characteristic feature of the small crystallite size compared to STO_C.

Average crystallite size (D) of the catalysts was determined using Scherrer equation as follows

$$D = \frac{0.9\lambda}{\beta \cos \theta} \quad (1)$$

where λ is the X-ray wavelength (1.5418 Å), β is the full width at half maximum, and θ is the Bragg angle. The average crystallite size evaluated from XRD patterns was found to be 63.5 and 37.4 nm for STO_C and STO_M, respectively. The average crystallite size of STO_M was found to be less and half the crystallite size of STO_C. This was due to microwave heating as it was reported that during microwave heating, the dipole change of the polar molecules takes place which leads to molecular agitation and friction and results in smaller particle size.³²

Rietveld Refinement Analysis. Rietveld refinement was performed using powder XRD data to obtain the structural

information. The parameters that are refined are scale factor, background, profile half-width parameters (u , v , and w), preferred orientation, isotropic displacement parameters, lattice parameters, isothermal temperature factors (B_{iso}), and atomic functional positions. Figure 2 illustrates the observed, calculated, and the difference in XRD patterns of STO nanocatalysts. Rietveld refinement analysis reveals that STO_C and STO_M have cubic $SrTiO_3$ phase.

The results obtained by the Rietveld refinement analysis showed good correlation between the observed/experimental XRD patterns and the calculated XRD patterns. However, small differences were found between the observed values (Y_{obs}) and calculated values (Y_{calc}) on the intensity scale near zero, as illustrated by the ($Y_{obs} - Y_{calc}$) line. The XRD data structure refinement of STO nanocatalysts are shown in Table 1. The values of fit parameters, χ^2 reveals the goodness-of-fit of refinement parameters, R_{wp} suggests the success of the refinement, and R_{Bragg} is the crystallographic model that was used to fit the experimental data, suggesting that the refinement results are very reliable. Further, it was observed that the STO_M catalyst has χ^2 less than STO_C, which confirms the phase purity in STO_M.

FTIR Spectroscopy. The FTIR spectra of the STO nanocatalysts measured at room temperature from 360 to 4000 cm^{-1} are shown in Figure 3a. The less intense band observed between 370 and 430 cm^{-1} in both of the catalysts was due to the TiO_{II} bending vibrations, and the absorption band in the range of about 500–800 cm^{-1} corresponds to the vibrations of Ti–O bond within the TiO_{VI} group.²⁰

Determination of Total Acidity and Acidic Strength of the Catalysts. Total acidity of the catalysts was determined by pyridine adsorption method by using FT-IR spectroscopy, and the corresponding FT-IR spectra of the STO_C and STO_M catalysts are presented in Figure 3b, and the results are given in Table 2. The two bands that appeared at 1433 and 1635 cm^{-1} in the FTIR spectra of the catalysts were assigned to pyridine chemisorbed to Lewis acid sites on the surface. In addition, the amount of Lewis acidity for STO_C (Table 2) was found to be 356 $\mu mol/g$ and for STO_M, it was found to be 363 $\mu mol/g$. The acidity results reveal that there is an increase in the number of Lewis acid sites in the catalyst synthesized by MH method compared to the CO method.

Acidic strength obtained by *n*-butylamine titration method is expressed as E (mV) and is given in Table 2. It was observed that E_i values of both of the catalysts were greater than 100 mV, which indicates the presence of strong or very strong acid

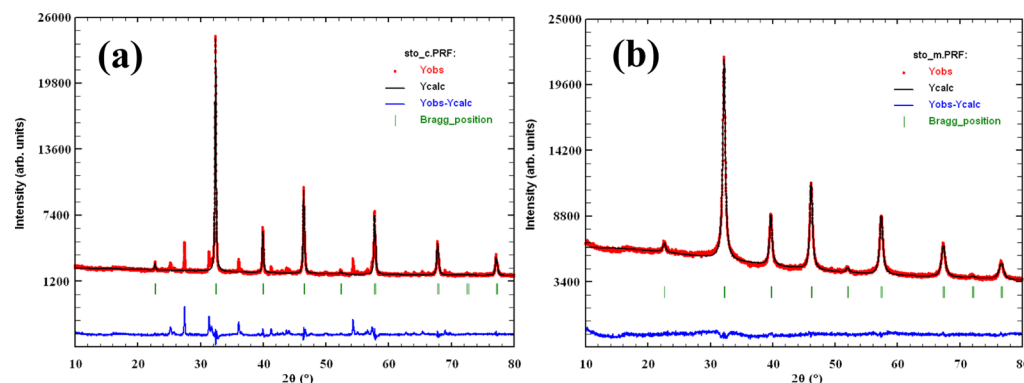
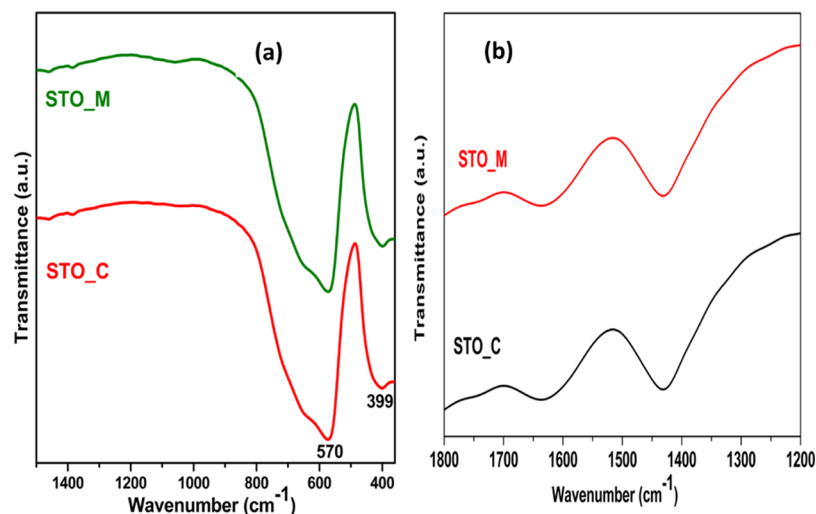


Figure 2. Observed, calculated, and the difference XRD patterns of (a) STO_C and (b) STO_M.

Table 1. Rietveld-Refined Structural Parameters for STO_C and STO_M Nanocatalysts

catalysts	space group	lattice parameters (Å)		cell volume (Å ³)	R_p	R_{wp}	R_{exp}	R_{Bragg}	R_f	χ^2
		a	c							
STO_C	$Pm\bar{3}m$	3.9076(2)	3.9076(2)	59.668(3)	3.84	6.04	2.13	5.76	5.65	8.02
STO_M	$Pm\bar{3}m$	3.9317(3)	3.9317(3)	60.779(2)	1.69	2.14	1.40	4.79	3.27	2.35

**Figure 3.** (a) FTIR spectra of fresh STO nanocatalysts synthesized by CO and MH methods. (b) FTIR spectra of adsorbed pyridine on STO nanocatalysts synthesized by CO and MH methods.**Table 2.** Acidic Strength and Total Acidity of the Synthesized Catalysts

catalysts	acidity by <i>n</i> -butylamine (E (mV))	acidity by pyridine adsorption ($\mu\text{mol/g}$)
STO_C	208	356
STO_M	241	363

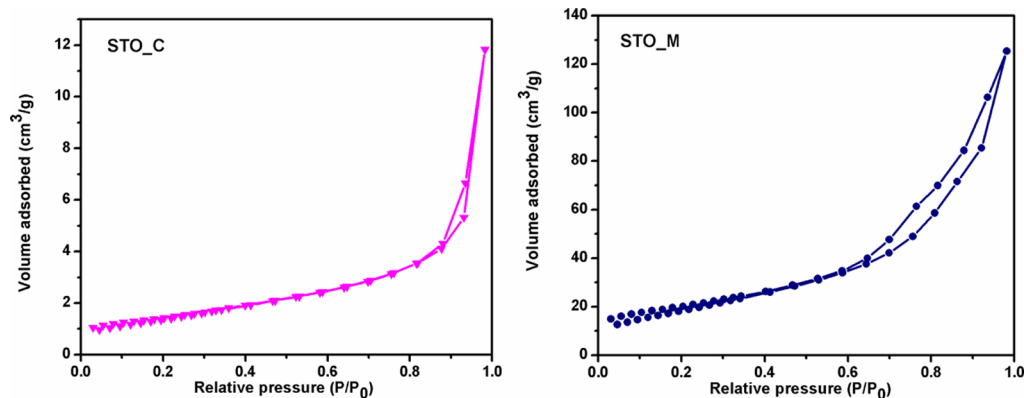
sites in the catalysts, and the acidic strength of the STO_M catalysts was higher than that of STO_C catalyst. This clearly indicates that microwave heating of the catalysts also enhanced the strength of acid sites.

BET Surface Area Analysis. As it was known that catalytic activity is strongly influenced by the surface properties, the same has been determined for the synthesized nanocatalysts by N₂ physisorption, and adsorption–desorption isotherms are shown in Figure 4. It was observed that both STO_M and STO_C showed a type IV isotherm which is a characteristic of

mesoporous materials along with H3 type H3 hysteresis loop in the range of 0.7–0.9 P/P_0 . STO_M catalyst showed a sharp increase in the N₂ adsorption step at a higher P/P_0 value (~ 0.7) with a large hysteresis loop compared to STO_C catalyst. Type H3 hysteresis loop indicates the presence of aggregates of particles giving rise to slit-shaped pores.³³ The specific surface area, pore volume, and pore diameter of the synthesized nanocatalysts are summarized in Table 3, and it

Table 3. BET Surface Area, Pore Volume, and Pore Diameter of the Catalysts from N₂ Adsorption–Desorption Studies and Particle Size from TEM and XRD Data

catalysts	BET surface area (m ² /g)	pore volume (cm ³ /g)	pore diameter (nm)	TEM particle size (nm)	XRD crystallite size (nm)
STO_C	5.11	0.01	8.0	102	63.5
STO_M	69.01	0.16	9.6	21.4	37.4

**Figure 4.** N₂ adsorption–desorption isotherm plots for STO nanocatalysts synthesized by the CO and MH methods.

was observed that BET surface area of the STO_M has 14 times high surface area compared to that of STO_C catalyst. The pore volume and pore diameter of the nanocatalysts also increased significantly in the STO_M nanocatalyst. The pore size of the synthesized nanocatalysts is greater than 2 nm, and it confirms the presence of mesopores in the catalysts.

Transmission Electron Microscopic Studies. Morphology and particle size of the catalysts were studied using transmission electron microscopy (TEM), and the images are displayed in Figure 5. It was observed that STO_C contains

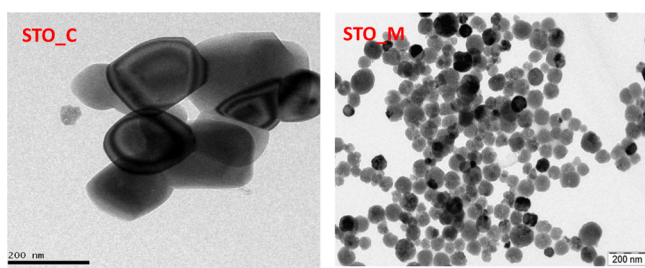


Figure 5. Transmission electron microscopy images of the STO catalysts.

large cubic particles and are highly agglomerated having an average particle size of 102 nm (Table 3). Whereas STO_M showed uniformly dispersed small spherical particles with an average particle size of 21.4 nm, which was much less compared to STO_C catalyst. Small particle size of the microwave catalyst was due to cavitation effect of microwave heating that has been discussed thoroughly in our previous paper.¹⁴ The decrease in particle size of the catalysts is in agreement with the XRD crystallite size (Table 3).

Figure 6 illustrates the high-resolution TEM images of the STO_M catalysts. Clear lattice fringes are observed, and the interlayer spacing calculated is 0.276 nm, as shown in Figure 6 (top) corresponding to the (110) crystal plane spacing of cubic SrTiO₃ (JCPDS card no. 073-0661, $d_{110} = 0.276$ nm). Energy-dispersive X-ray (EDX) spectra of STO_M catalysts are shown

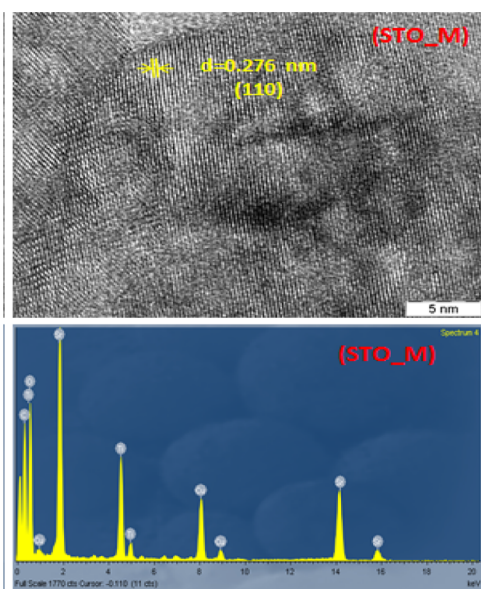


Figure 6. High-resolution TEM images showing the lattice fringes (top) and EDX spectra (bottom) of STO_M catalysts.

in Figure 6 (bottom). EDX analysis reveals the presence of Sr, Ti, and O in STO_M catalysts.

Catalytic Activity Studies. Catalytic performance of the STO_M and STO_C catalysts has been evaluated for various reactions which are discussed in detail below. We have performed blank reactions for all of the three reactions and observed no reactivity in the absence of catalyst.

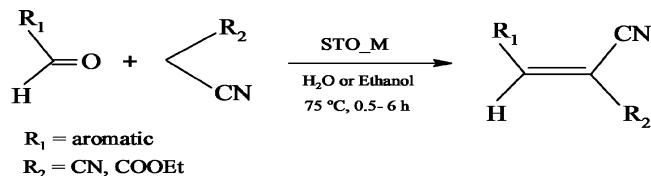
Knoevenagel Condensation. Catalytic activity of the synthesized catalysts was evaluated for Knoevenagel condensation reaction using benzaldehyde and ethylcyanoacetate as reactants with ethyl α -cyanocinnamate yielded as the major product. All of the products are identified using GC-MS. The catalytic activities of the STO catalysts synthesized by CO and MH methods are compared and is shown in Table 4. Both

Table 4. Catalytic Activity Results of STO Catalysts for Knoevenagel Condensation, Catalytic Transfer Hydrogenation, and Amination Reactions

type of catalyst	conversion (%)	selectivity (%)	yield (%)	time (min)
Knoevenagel Condensation Reaction of Benzaldehyde with Ethylcyanoacetate				
STO_C	100	100	100	35
STO_M	100	100	100	15
type of catalyst	conversion (%)	selectivity (%)	yield (%)	time (h)
Catalytic Transfer Hydrogenation of Nitrobenzene				
STO_C	95.7	100	91.6	1
STO_M	100	100	100	1
Amination of Benzaldehyde with Aniline				
STO_C	96	82	78	24
STO_M	100	99.6	99.6	23

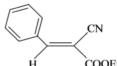
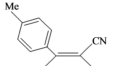
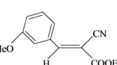
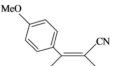
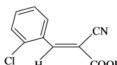
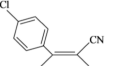
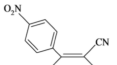
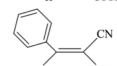
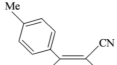
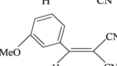
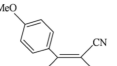
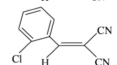
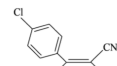
STO catalysts showed 100% conversion as well as 100% selectivity toward the formation of ethyl α -cyanocinnamate. In particular, STO_M catalyst showed conversion (100%) in less time within 15 min. This was due to improved physical properties such as surface area, pore diameter, and pore volume of STO_M catalysts (see Table 3) because of microwave heating. Because the rate of condensation of benzaldehyde and ethyl cyanoacetate was faster on STO_M, the study was extended further with this catalyst on another active methylene compound, malononitrile (Scheme 1). The

Scheme 1. Knoevenagel Condensation Reaction of Aromatic Aldehydes with Active Methylene Compounds



STO_M catalyst was also found to be highly effective for benzaldehyde condensation with malononitrile and resulted in 100% yield of the product within 30 min reaction time (Table 5, entry 8). Good yields with ethyl cyanoacetate and malononitrile in short time could be because of presence of the electron-withdrawing group, which facilitates easy release of protons from active methylene groups and stabilizes the negative charge through resonance (enolate formation).³⁴ The effect of the substitution in the benzaldehyde was studied with both ethylcyanoacetate and malononitrile with similar reaction conditions (Table 5). All of the substituted benzaldehyde

Table 5. Results of Knoevenagel Condensation Reaction of Substituted Benzaldehyde with Ethyl Cyanoacetate and Malononitrile Over STO_M Catalyst^a

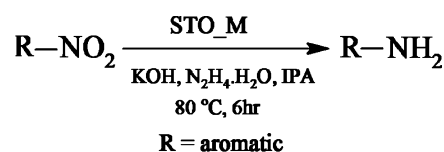
S. No.	Aldehyde	Active methylene compound	Product	Time (h)	Conversion (%)	Selectivity (%)
1	Benzaldehyde	Ethyl cyanoacetate		0.25	100	100
2	4-Methylbenzaldehyde	Ethyl cyanoacetate		1	91.3	92.8
3	3-Methoxybenzaldehyde	Ethyl cyanoacetate		2	99.9	100
4	4-Methoxybenzaldehyde	Ethyl cyanoacetate		1	89.2	86.6
5	2-Chlorobenzaldehyde	Ethyl cyanoacetate		1	99.2	100
6	4-Chlorobenzaldehyde	Ethyl cyanoacetate		1	100	97.7
7	4-Nitrobenzaldehyde	Ethyl cyanoacetate		6	100	41.2
8	Benzaldehyde	Malononitrile		0.33	100	100
9	4-Methylbenzaldehyde	Malononitrile		6	56.9	100
10	3-Methoxybenzaldehyde	Malononitrile		3	66.5	100
11	4-Methoxybenzaldehyde	Malononitrile		6	72.3	100
12	2-Chlorobenzaldehyde	Malononitrile		1	55.3	98.4
13	4-Chlorobenzaldehyde	Malononitrile		2	72.3	100

^aReaction conditions: 120 mg of STO_M catalyst, 20 mmol of aldehyde, 20 mmol of active methylene compound, 10 mL of deionized water, and 20 mL of ethanol, refluxed at 75 °C.

compounds having electron-withdrawing as well as electron-donating groups have shown remarkable good yields for ethyl

cyanoacetate and, in the case of malononitrile, all substituted benzaldehyde compounds showed less conversions (55–72%) in 3–6 h (Table 5, entry 9–13). This could be because of the decrease in the electrophilicity on the active center of the benzaldehyde.³⁵ Table 6 shows the comparison of the catalytic activity of STO_M catalyst with other catalysts that are reported in the literature for Knoevenagel condensation of benzaldehyde with active methylene compounds. These studies reveal that STO_M catalyst in the present study has showed 100% conversion and selectivity for condensation of benzaldehyde with ethylcyanoacetate and malononitrile in less than 30 min compared to the reported systems. Moreover, STO is inexpensive and economical compared to most of the catalysts given in Table 6.

Catalytic Transfer Hydrogenation. We have also investigated the catalytic performance of the catalysts for catalytic transfer hydrogenation of nitrobenzene to aniline in the presence of hydrazine hydrate as the hydrogen donor. Scheme 2 depicts a typical catalytic transfer hydrogenation of

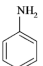
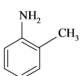
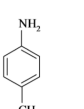
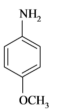
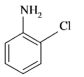
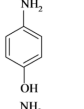
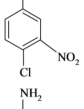
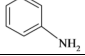
Scheme 2. Catalytic Transfer Hydrogenation of Nitroarenes with Hydrazine Hydrate

nitroarenes to the corresponding amines. In this reaction, aniline was yielded as the major product. Table 4 shows the catalytic activity of the catalysts. Compared with STO_C catalyst, STO_M catalyst showed 100% nitrobenzene conversion with 100% aniline selectivity. Furthermore, catalytic activity of STO_M for substituted nitrobenzene substrates has been studied under similar reaction conditions (Table 7). It was observed that para-substituted compounds gave very good yields, whereas for ortho-substituted compounds' yields are very less, which could be attributed to steric hindrance (Table 7, entry 2, 5, 7). Table 8 shows the comparison of catalytic activity of STO_M catalyst with the reported systems in literature for catalytic transfer hydrogenation of nitrobenzene to aniline. Our catalyst performance is comparable with most of the reported catalysts including our previous studies.¹⁴ The only difference observed is that few reported catalytic systems are highly expensive, and scarcity of these metals makes the

Table 6. Comparison of Activity of STO_M Catalyst with the Reported Catalysts for the Knoevenagel Condensation of Benzaldehyde with Malononitrile or Ethylcyanoacetate

s. no.	catalyst	temperature (°C)	solvent	ethylcyano acetate		malononitrile		refs
				time (h)	yield (%)	time (h)	yield (%)	
1	TMU-5 (MOFs)	RT	H ₂ O			0.5	100	5
2	borated zirconia	RT	solvent free	0.25	99	0.5	98	34
3	Zn β zeolite	140	solvent free	6	72	6	16.1	36
4	Na-SBA-1	190	solvent free	24	82			37
5	CoFe ₂ O ₄	50	ethanol/H ₂ O	0.42	95			38
6	Ti-TUD-1	RT	ethanol	1.2	82	0.5	91	39
7	Ce _x Zr _{1-x} O ₂	80	ethanol	1.25	78	0.83	82	40
8	InCl ₃	60	toluene/AC ₂ O			8	94	26
9	KOH/La ₂ O ₃ -MgO	RT	solvent free	3	95	0.25	99.5	41
10	SrTiO ₃	75	ethanol/H ₂ O	0.25	100	0.5	100	present work

Table 7. Catalytic Transfer Hydrogenation of Substrates of Nitrobenzene over STO_M Catalyst^a

S. No.	Substrate	Product	Time (h)	Conversion (%)	Selectivity (%)
1	Nitrobenzene		1	100	100
2	2-Nitrotoluene		6	32.6	94.6
3	4-Nitrotoluene		4	91.2	100
4	4-Nitroanisole		5	100	100
5	2-Chloronitrobenzene		6	100	63.8
6	4-Nitrophenol		10	0.07	100
7	2,4-Dinitrochlorobenzene		6	57.9	76
8	3-Nitroaniline		6	78	100

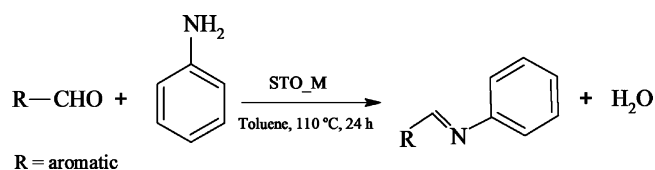
^aReaction conditions: 80 mg of STO_M catalyst, 10 mmol of substrate, 10 mmol of KOH, 1.5 mL of hydrazine hydrate, 10 mL of propan-2-ol (IPA), refluxed at 80 °C.

Table 8. Comparison of Activity of STO_M Catalyst with the Reported Catalysts for Reduction of Nitrobenzene to Aniline (Hydrazine Hydrate as a Hydrogen Donor)

s. no.	catalyst	temperature (°C)	yield (%)	refs
1	iron oxide hydroxide		98	42
2	reduced graphene oxide	30	97.4	43
3	Fe-phenanthroline/C	100	99	44
4	Au/TiO ₂	60	92	45
5	Pd-gCN	70	99	46
6	BaTiO ₃	80	100	14
7	SrTiO ₃	80	100	present study

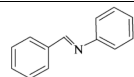
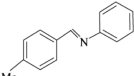
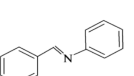

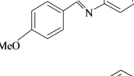
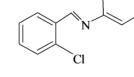
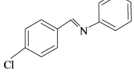
process costly compared to our green, economical, and multitasking STO catalyst.

Amination of Benzaldehyde. The catalytic activity of the synthesized catalysts toward amination of benzaldehyde is also discussed here. Scheme 3 depicts a typical amination of

Scheme 3. Amination of Benzaldehyde Using STO Catalysts

benzaldehyde using aniline on synthesized catalysts. In this reaction, Schiff bases yielded as the major product. Compared with STO_C catalyst, the STO_M catalyst showed 100% conversion with 99.6% selectivity toward the formation of a Schiff base (Table 4). The effect of the substitution at para, meta, and ortho positions of benzaldehyde on amination reaction was studied with STO_M catalyst under similar reaction conditions (Table 9). Interestingly, substituted

Table 9. Amination of Substituted Benzaldehyde over STO_M Catalyst^a

S. No.	Aldehyde	Product	Conversion (%)	Selectivity (%)
1	Benzaldehyde		100	99.6
2	4-Methylbenzaldehyde		100	100
3	3-Methoxybenzaldehyde		92.2	100
4	4-Methoxybenzaldehyde		97	100
5	2-Chlorobenzaldehyde		100	100
6	4-Chlorobenzaldehyde		94.1	100
7	4-Nitrobenzaldehyde		72	100

^aReaction conditions: 120 mg of STO_M catalyst, 2 mmol of benzaldehyde, 2 mmol of aniline, and 2 mL of toluene refluxed at 110 °C for 24 h.

benzaldehydes did not affect the yield of Schiff bases much. Table 10 shows the comparison of catalytic activity of STO_M catalyst with the reported catalysts in literature for amination of benzaldehyde with aniline. Our catalyst has showed 100% yield, whereas the reported catalysts showed less yields at variable reaction conditions. In the present study, we have revealed STO_M catalyst as one of the prominent multitasking

Table 10. Comparison of Activity of STO_M Catalyst with the Reported Catalysts for Amination of Benzaldehyde with Aniline

s. no.	catalytic system	temperature (°C)	yield %	refs
1	P ₂ O ₅ /SiO ₂	RT	85	47
2	P ₂ O ₅ /Al ₂ O ₃	RT	80	48
3	[bmim]PF ₆		94	49
4	erbium(III) triflate	RT	67	50
5	TiO ₂	RT	98	51
6	montmorillonite	RT	95	52
7	SrTiO ₃	reflux	100	present work

catalyst, by its application for Knoevenagel condensation, catalytic transfer hydrogenation, and amination reactions.

Recyclability of the STO Catalyst. STO_M was selected for testing the recyclability capability for the above three reactions because this catalyst showed superior catalytic performance compared to STO_C. It was found that it could be reused without significant loss in the catalytic activity up to three reaction cycles.

CONCLUSIONS

In conclusion, we have synthesized pure SrTiO₃ nanocatalyst by using microwave hydrothermal method, which exhibits good textural and surface properties compared to conventionally synthesized catalyst and has proven highly efficient for the synthesis of amines, imines, and α , β -unsaturated carbonyl compounds via catalytic transfer hydrogenation, amination, and Knoevenagel condensation reactions. Rietveld analysis of the XRD data confirmed SrTiO₃ crystallize in cubic structure. Traces of carbonate and TiO₂ impurities are present in the XRD of conventional catalyst, whereas pure phase without any impurities was obtained in microwave-synthesized catalyst. Average particle size of the microwave catalyst determined from TEM image was found to be 21.4 which is much less compared to conventional catalyst particle size of 102 nm. Both the conventional and microwave-synthesized SrTiO₃ catalysts showed good reactivity for all of the three reactions chosen in the present study. However, excellent catalytic performance of the microwave SrTiO₃ catalyst was due to the high surface area, Lewis acidity, and high acidic strength of the catalyst compared to a conventional one. Almost 100% conversion with >99.6% selectivity has been observed on microwave SrTiO₃ catalyst in all of the reactions, where it has been applied except in few cases of substituted substrates. In short, synthesis of SrTiO₃ catalyst in pure form by microwave-hydrothermal method containing excellent catalytic properties is achieved at low synthesis temperature and in less time makes the process green, energy efficient, and environmentally friendly compared to its counter high-temperature conventional catalyst. The present study also marks the first-time application of SrTiO₃ as an efficient multitask catalyst, which can be used potentially as a cost-effective industrial catalyst.

EXPERIMENTAL SECTION

Synthesis of SrTiO₃ Nanocatalysts. *CO Method.* SrTiO₃ nanoparticles were synthesized using titanium isopropoxide (Ti (OC₃H₇)₄), strontium nitrate (Sr (NO₃)₂) as precursors, oxalic acid (C₂H₂O₄·2H₂O) as a chelating agent, and 2-propanol (C₃H₇OH) as the solvent. The molar composition of the precursors are as follows: Sr (NO₃)₂/Ti (OC₃H₇)₄/C₂H₂O₄·2H₂O = 1:1:2. Aqueous solutions of strontium nitrate and oxalic acid are added to titanium isopropoxide solution separately dissolved in 50 mL of 2-propanol and water, and the mixture solution was stirred at 60 °C for 1 h and the homogenous solution thus obtained was evaporated to dryness at 100 °C. The solid precursor thus obtained was dried at 120 °C overnight in the oven, and the dried sample was ground to a fine powder and calcined at 900 °C for 12 h in a static air furnace.

MH Method. SrCl₂·2H₂O and titanium tetrachloride (TiCl₄) were chosen as starting materials for the synthesis of SrTiO₃. In a typical synthesis of SrTiO₃, TiCl₄ was added to the distilled water at 0 °C to this aqueous solution of SrCl₂.

2H₂O was added and stirred for some time and KOH was added while stirring and a homogenous solution was obtained. The molar ratio of the precursors maintained at TiCl₄/SrCl₂·2H₂O/KOH/H₂O is 1:2:30:300. The homogenous solution thus obtained was transferred to Teflon-lined autoclave and placed the same in the microwave instrument at 180 °C and treated for 30 min (Model: MW 5000, SINEO, maximum power of 1500 W). The autoclave thus cooled to room temperature after treatment, and the solid product obtained was washed with 0.1 M aqueous acetic acid solution and deionized water. The solid product was recovered by centrifugation and dried at 105 °C overnight.

AUTHOR INFORMATION

Corresponding Author

*E-mail: ch.srilakshmi@gmail.com, chilukotis@iisc.ac.in.
Phone. +91 080 43365821 (C.S.).

ORCID

Chilukoti Srilakshmi: 0000-0001-6660-8746

Notes

The authors declare no competing financial interest.

ACKNOWLEDGMENTS

This work was financially supported by Department of Science and Technology (DST), India, through INSPIRE project. C.S.L. would like to thank Prof. Ramasesha and Prof. A. K. Shukla for their encouragement and support in carrying out this work.

REFERENCES

- (1) Wang, H.; Li, L.; Bai, X.-F.; Deng, W.-H.; Zheng, Z.-J.; Yang, K.-F.; Xu, L.-W. One-by-one hydrogenation, cross-coupling reaction, and Knoevenagel condensations catalyzed by PdCl₂ and the downstream palladium residue. *Green Chem.* **2013**, *15*, 2349–2355.
- (2) Pyun, J. Graphene oxide as catalyst: Application of carbon materials beyond nanotechnology. *Angew. Chem., Int. Ed.* **2011**, *50*, 46–48.
- (3) Saptal, V. B.; Bhanage, B. M. Bifunctional ionic liquids for the multitask fixation of carbon dioxide into valuable chemicals. *ChemCatChem* **2016**, *8*, 244–250.
- (4) Tavakkoli, H.; Sanaeishoar, H.; Mohave, F.; Nouroozi, Z.; Moeinirad, M. Catalytic application of some perovskite nano-oxides for the one-pot synthesis of 1,8-dioxodecahydroacridines. *React. Kinet., Mech. Catal.* **2016**, *119*, 259–272.
- (5) Masoomi, M. Y.; Beheshti, S.; Morsali, A. Mechanochemical synthesis of new azine-functionalized Zn(II) metal-organic frameworks for improved catalytic performance. *J. Mater. Chem. A* **2014**, *2*, 16863–16866.
- (6) Motokura, K.; Baba, T. An atom-efficient synthetic method: carbosilylations of alkenes, alkynes, and cyclic acetals using Lewis and Brønsted acid catalysts. *Green Chem.* **2012**, *14*, 565–579.
- (7) Varadwaj, G. B. B.; Rana, S.; Parida, K. M. Amine functionalized K10 montmorillonite: A solid acid-base catalyst for the Knoevenagel condensation reaction. *Dalton Trans.* **2013**, *42*, 5122–5129.
- (8) García-Verdugo, E.; Altava, B.; Burguete, M. I.; Lozano, P.; Luis, S. V. Ionic liquids and continuous flow processes: A good marriage to design sustainable processes. *Green Chem.* **2015**, *17*, 2693–2713.
- (9) Dapsens, P. Y.; Mondelli, C.; Kusuma, B. T.; Verel, R.; Pérez-Ramírez, J. A continuous process for glyoxal valorisation using tailored Lewis-acid zeolite catalysts. *Green Chem.* **2014**, *16*, 1176–1186.
- (10) Verboeckend, D.; Nuttens, N.; Locus, R.; Van Aelst, J.; Verolme, P.; Groen, J. C.; Pérez-Ramírez, J.; Sels, B. F. Synthesis, characterisation, and catalytic evaluation of hierarchical faujasite zeolites: Milestones, challenges, and future directions. *Chem. Soc. Rev.* **2016**, *45*, 3331–3352.

- (11) Reinsch, H.; Stock, N. Synthesis of MOFs: A personal view on rationalisation, application and exploration. *Dalton Trans.* **2017**, *46*, 8339–8349.
- (12) Ding, L.; Li, H.; Zhang, Y.; Zhang, K.; Yuan, H.; Wu, Q.; Zhao, Y.; Jiao, Q.; Shi, D. Basic polymerized imidazolidine-based ionic liquid: An efficient catalyst for aqueous Knoevenagel condensation. *RSC Adv.* **2015**, *5*, 21415–21421.
- (13) Ying, A.; Liang, H.; Zheng, R.; Ge, C.; Jiang, H.; Wu, C. A simple, efficient, and green protocol for Knoevenagel condensation in a cost-effective ionic liquid 2-hydroxyethylammonium formate without a catalyst. *Res. Chem. Intermed.* **2011**, *37*, 579–585.
- (14) Srilakshmi, C.; Saraf, R.; Prashanth, V.; Rao, G. M.; Shivakumara, C. Structure and Catalytic Activity of Cr-Doped BaTiO₃ Nanocatalysts Synthesized by Conventional Oxalate and Microwave Assisted Hydrothermal Methods. *Inorg. Chem.* **2016**, *55*, 4795–4805.
- (15) Hu, M. Z.-C.; Miller, G. A.; Payzant, E. A.; Rawn, C. J. Homogeneous (co)precipitation of inorganic salts for synthesis of monodispersed barium titanate particles. *J. Mater. Sci.* **2000**, *35*, 2927–2936.
- (16) Liu, X.; Bai, H. Liquid-solid reaction synthesis of SrTiO₃ submicron-sized particles. *Mater. Chem. Phys.* **2011**, *127*, 21–23.
- (17) Rabuffetti, F. A.; Kim, H.-S.; Enterkin, J. A.; Wang, Y.; Lanier, C. H.; Marks, L. D.; Poeppelmeier, K. R.; Stair, P. C. Synthesis-Dependent First-Order Raman Scattering in SrTiO₃Nanocubes at Room Temperature. *Chem. Mater.* **2008**, *20*, 5628–5635.
- (18) Hernandez, B. A.; Chang, K.-S.; Fisher, E. R.; Dorhout, P. K. Sol–Gel Template Synthesis and Characterization of BaTiO₃ and PbTiO₃ Nanotubes. *Chem. Mater.* **2002**, *14*, 480–482.
- (19) Yang, J.; Zhang, J.; Liang, C.; Wang, M.; Zhao, P.; Liu, M.; Liu, J.; Che, R. Ultrathin BaTiO₃ Nanowires with High Aspect Ratio: A Simple One-Step Hydrothermal Synthesis and Their Strong Microwave Absorption. *ACS Appl. Mater. Interfaces* **2013**, *5*, 7146–7151.
- (20) Srilakshmi, C.; Rao, G. M.; Saraf, R. Effect of the nature of a transition metal dopant in BaTiO₃ perovskite on the catalytic reduction of nitrobenzene. *RSC Adv.* **2015**, *5*, 45965–45973.
- (21) Vekariya, R. H.; Patel, H. D. Recent advances in the synthesis of coumarin derivatives via Knoevenagel condensation: A review. *Synth. Commun.* **2014**, *44*, 2756–2788.
- (22) Seto, H.; Imai, K.; Hoshino, Y.; Miura, Y. Polymer microgel particles as basic catalysts for Knoevenagel condensation in water. *Polym. J.* **2016**, *48*, 897–904.
- (23) Gao, Z.; Zhou, J.; Cui, F.; Zhu, Y.; Hua, Z.; Shi, J. Superparamagnetic mesoporous Mg-Fe Bi-metal oxides as efficient magnetic solid-base catalysts for Knoevenagel condensations. *Dalton Trans.* **2010**, *39*, 11132–11135.
- (24) Li, G.; Xiao, J.; Zhang, W. Efficient and reusable amine-functionalized polyacrylonitrile fiber catalysts for Knoevenagel condensation in water. *Green Chem.* **2012**, *14*, 2234–2242.
- (25) Hangarge, R. V.; Jarikote, D. V.; Shingare, M. S. Knoevenagel condensation reactions in an ionic liquid. *Green Chem.* **2002**, *4*, 266–268.
- (26) Ogiwara, Y.; Takahashi, K.; Kitazawa, T.; Sakai, N. Indium(III)-catalyzed Knoevenagel condensation of aldehydes and activated methylenes using acetic anhydride as a promoter. *J. Org. Chem.* **2015**, *80*, 3101–3110.
- (27) Panigrahi, S.; Basu, S.; Praharaj, S.; Pande, S.; Jana, S.; Pal, A.; Ghosh, S. K.; Pal, T. Synthesis and Size-Selective Catalysis by Supported Gold Nanoparticles: Study on Heterogeneous and Homogeneous Catalytic Process. *J. Phys. Chem. C* **2007**, *111*, 4596–4605.
- (28) Patil, R. D.; Adimurthy, S. Catalytic methods for imine synthesis. *Asian J. Org. Chem.* **2013**, *2*, 726–744.
- (29) Barluenga, J.; Aznar, F.; Valdés, C. N-Trialkylsilylimines as Coupling Partners for Pd-Catalyzed C–N Bond-Forming Reactions: One-Step Synthesis of Imines and Azadienes from Aryl and Alkenyl Bromides. *Angew. Chem., Int. Ed.* **2004**, *43*, 343–345.
- (30) Morales, S.; Guijarro, F. G.; García Ruano, J. L.; Cid, M. B. A general aminocatalytic method for the synthesis of aldimines. *J. Am. Chem. Soc.* **2014**, *136*, 1082–1089.
- (31) Srilakshmi, C.; Saraf, R. Ag-doped hydroxyapatite as efficient adsorbent for removal of Congo red dye from aqueous solution: Synthesis, kinetic and equilibrium adsorption isotherm analysis. *Microporous Mesoporous Mater.* **2016**, *219*, 134–144.
- (32) Mohajerani, M. S.; Mazlumi, M.; Lak, A.; Kajbafvala, A.; Zanganeh, S.; Sadrezaad, S. K. Self-assembled zinc oxide nanostructures via a rapid microwave-assisted route. *J. Cryst. Growth* **2008**, *310*, 3621–3625.
- (33) Sing, K. S. W.; Everett, D. H.; Haul, R. A. W.; Moscou, L.; Pierotti, R. A.; Rouquerol, J.; Siemieniewska, T. Reporting physisorption data for gas/solid systems with special reference to the determination of surface area and porosity. *Pure Appl. Chem.* **1985**, *57*, 603–619.
- (34) Sinhamahapatra, A.; Pal, P.; Tarafdar, A.; Bajaj, H. C.; Panda, A. B. Mesoporous borated zirconia: A solid acid-base bifunctional catalyst. *ChemCatChem* **2013**, *5*, 331–338.
- (35) Sarmah, B.; Satpati, B.; Srivastava, R. Highly efficient and recyclable basic mesoporous zeolite catalyzed condensation, hydroxylation, and cycloaddition reactions. *J. Colloid Interface Sci.* **2017**, *493*, 307–316.
- (36) Saravanamurugan, S.; Palanichamy, M.; Hartmann, M.; Murugesan, V. Knoevenagel condensation over β and γ zeolites in liquid phase under solvent free conditions. *Appl. Catal., A* **2006**, *298*, 8–15.
- (37) Yang, H.; Li, J.; Zhang, H.; Lv, Y.; Gao, S. Facile synthesis of POM@MOF embedded in SBA-15 as a steady catalyst for the hydroxylation of benzene. *Microporous Mesoporous Mater.* **2014**, *195*, 87–91.
- (38) Senapati, K. K.; Borgohain, C.; Phukan, P. Synthesis of highly stable CoFe₂O₄ nanoparticles and their use as magnetically separable catalyst for Knoevenagel reaction in aqueous medium. *J. Mol. Catal. A: Chem.* **2011**, *339*, 24–31.
- (39) Karmakar, B.; Chowdhury, B.; Banerji, J. Mesoporous titanate Ti-TUD-1 catalyzed Knoevenagel reaction: An efficient green synthesis of trisubstituted electrophilic olefins. *Catal. Commun.* **2010**, *11*, 601–605.
- (40) Postole, G.; Chowdhury, B.; Karmakar, B.; Pinki, K.; Banerji, J.; Auroux, A. Knoevenagel condensation reaction over acid-base bifunctional nanocrystalline CexZr1-xO₂ solid solutions. *J. Catal.* **2010**, *269*, 110–121.
- (41) Wei, Y.; Zhang, S.; Yin, S.; Zhao, C.; Luo, S.; Au, C.-t. Solid superbase derived from lanthanum-magnesium composite oxide and its catalytic performance in the Knoevenagel condensation under solvent-free condition. *Catal. Commun.* **2011**, *12*, 1333–1338.
- (42) Shi, Q.; Lu, R.; Jin, K.; Zhang, Z.; Zhao, D. Simple and eco-friendly reduction of nitroarenes to the corresponding aromatic amines using polymer-supported hydrazine hydrate over iron oxide hydroxide catalyst. *Green Chem.* **2006**, *8*, 868–870.
- (43) Gao, Y.; Ma, D.; Wang, C.; Guan, J.; Bao, X. Reduced graphene oxide as a catalyst for hydrogenation of nitrobenzene at room temperature. *Chem. Commun.* **2011**, *47*, 2432–2434.
- (44) Jagadeesh, R. V.; Wienhöfer, G.; Westerhaus, F. A.; Surkus, A.-E.; Pohl, M.-M.; Junge, H.; Junge, K.; Beller, M. Efficient and highly selective iron-catalyzed reduction of nitroarenes. *Chem. Commun.* **2011**, *47*, 10972–10974.
- (45) Gkizis, P. L.; Stratakis, M.; Lykakis, I. N. Catalytic activation of hydrazine hydrate by gold nanoparticles: Chemoselective reduction of nitro compounds into amines. *Catal. Commun.* **2013**, *36*, 48–51.
- (46) Nandi, D.; Siwal, S.; Choudhary, M.; Mallick, K. Carbon nitride supported palladium nanoparticles: An active system for the reduction of aromatic nitro-compounds. *Appl. Catal., A* **2016**, *523*, 31–38.
- (47) Naeimi, H.; Sharghi, H.; Salimi, F.; Rabiei, K. Facile and efficient method for preparation of Schiff bases catalyzed by P₂O₅/SiO₂ under free solvent conditions. *Heteroat. Chem.* **2008**, *19*, 43–47.
- (48) Naeimi, H.; Salimi, F.; Rabiei, K. Mild and convenient one pot synthesis of Schiff bases in the presence of P₂O₅/Al₂O₃ as new

catalyst under solvent-free conditions. *J. Mol. Catal. A: Chem.* **2006**, *260*, 100–104.

(49) Andrade, C. K.; Suarez, P. A.; Takada, S. C.; Alves, L. M.; Rodrigues, J. P.; Brandão, R. F.; Soares, V. C. Molecular sieves in ionic liquids as an efficient and recyclable medium for the synthesis of imines. *Synlett* **2004**, 2135–2138.

(50) Dalpozzo, R.; De Nino, A.; Nardi, M.; Russo, B.; Procopio, A. Erbium(III) triflate: A valuable catalyst for the synthesis of aldimines, ketimines, and enaminones. *Synthesis* **2006**, 1127–1132.

(51) Hosseini-Sarvari, M. Nano-tube TiO₂ as a new catalyst for eco-friendly synthesis of imines in sunlight. *Chin. Chem. Lett.* **2011**, *22*, 547–550.

(52) Naeimi, H.; Rabiei, K. Montmorillonite as a heterogeneous catalyst in the efficient, mild and one pot synthesis of schiff bases under solvent-free conditions. *J. Chin. Chem. Soc.* **2012**, *59*, 208–212.